Published paper

D. Zarko, S. Stipetic, M. Martinovic, M. Kovacic, T. Jercic and Z. Hanic, "Reduction of Computational Efforts in Finite Element-Based Permanent Magnet Traction Motor Optimization," in *IEEE Transactions on Industrial Electronics*, vol. 65, no. 2, pp. 1799-1807 Feb. 2018.

http://dx.doi.org/10.1109/TIE.2017.2736485

Reduction of Computational Efforts in Finite Element Based Permanent Magnet Traction Motor Optimization

Damir Zarko, *Member,* Stjepan Stipetic, *Member,* Marijan Martinovic, Marinko Kovacic, *Student Member,* Tino Jercic, *Student Member*, Zlatko Hanic, *Student Member*

***Abstract*—This paper presents a method for reducing computational time in constrained single objective optimization problems related to permanent magnet motors modeled using computationally intensive finite element method. The method is based on Differential Evolution algorithm. The principal approach is to interrupt the evaluation of inequality constraints after encountering the constraint which is violated and continue their evaluation only if better solutions are obtained in comparison with the candidate vector from the previous generation both in terms of inequality constraints and the cost function. This approach avoids unnecessary time consuming finite element calculations required for solving the inequality constraints and saves the overall optimization time without affecting the convergence rate. The main features of this approach and how it complements the existing method for handling inequality constraints in Differential Evolution algorithm is demonstrated on design optimization of an interior permanent magnet motor for the low-floor tram TMK 2200. The motor geometry is optimized for maximum torque density.**

Keywords: optimization, constraints, electric tram, traction motor, permanent magnet synchronous motor, electromagnetic design, differential evolution

I. Introduction

THE application of optimization algorithms nowadays enjoys high popularity among electrical machine designers [1]–[8]. A visible shift of interest in optimization from academia towards manufacturers can be easily observed in worldwide scientific literature. Designer's experience in obtaining brilliant designs is not to be underestimated, but due to nonlinearity and complexity of the relations between the geometry of electrical machines and their performance, it is commonly understood that only the mathematical optimization can push the boundaries towards better designs.

This is especially noticeable in the problem of increasing efficiency [9]–[12] due to worldwide legislation initiatives. Boosting of efficiency in all types of electric drives in industry and transport has been made one of strategic goals of energy policy conducted in Europe, United States and elsewhere [13], [14]. The increase of efficiency can be achieved by increasing the size of existing motors and/or installing laminations with lower specific losses. Further improvement may be achieved with redesign of the geometry of existing motors by means of mathematical optimization.

Certain machine types inherently have a high computational load for the accurate calculation of the performance, such as interior permanent magnet motors (IPM) or synchronous reluctance motors (SynRM) [15], [16]. A research group around Ionel and Demerdash [17]–[22] invested their efforts in the reduction of the computational time by inventing methods to reduce calculation time per optimization candidate. On the other hand, Bramerdorfer et. al. [23] made a detailed analysis regarding the possibilities for speeding up the finite element (FE) based optimization of electrical machines with an emphasis on multistage analysis which is an improvement of the optimization procedure itself.

In the case of traction drives, the limited space available on the vehicle's bogie is always a restraining factor for the traction motor [24]. For traction applications, IPM fits naturally due to its torque-speed characteristic suitable for wide speed range in constant power mode of operation which can be tuned as required by proper design of the motor.

The motivation for this paper emerged in the research project which studied the possibility of replacing an existing induction motor driving a low floor tram with an IPM motor of the same volume, but with increased torque rating so that six induction motors can be replaced with four IPMs. This paper aims to reduce the overall computational time by defining a novel way of handling constraint functions in the differential evolution (DE) optimization algorithm which contain computationally intensive finite element based calculations.

II. Traction Motor requirements

An induction motor (IM) which drives the low-floor tram KONČAR TMK2200 is used in this research as a starting point for IPM motor design. The main idea is to replace the IM with the IPM motor and permit its assembly on the tram's bogie without additional modifications. This constraint requires both motors to have approximately the same outer dimensions. In addition, both machines are assumed to have the same shaft, bearings and cooling system which result in approximately the same friction and windage losses. The existing IM and the IPM prototype are compared in Fig. 1 showing the overall length of both machines and the lengths of the lamination stacks.

Damir Žarko, Stjepan Stipetić, Marinko Kovačić, Tino Jerčić, Zlatko Hanić are with the University of Zagreb Faculty of Electrical Engineering and Computing, Department of Electric Machines, Drives and Automation, Zagreb, Croatia (e-mail: stjepan.stipetic@fer.hr).

Marijan Martinović was a research associate on MAGEF project on the University of Zagreb. Currently with Elaphe, Ljubljana, Slovenia.

The outer dimensions and outline of the stator laminations are identical in both motors.

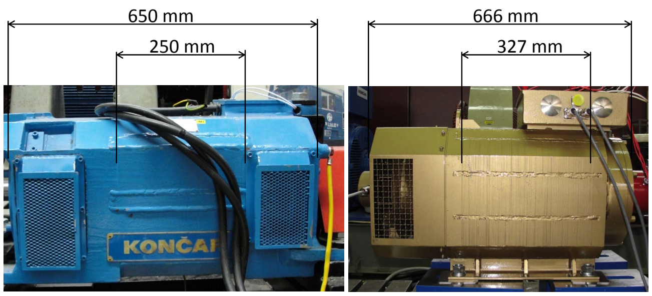

Fig. 1. Size comparison of induction motor for low-floor tram TMK2200 (left image) and IPM prototype (right image)

Tramcar series TMK2200 is driven by six 3-phase 4-pole squirrel-cage induction motors with the following ratings for maximum load during acceleration: 85 kW, 320 V, 195 A, 477 Nm, 1700 min^{-1}. The maximum speed is 4580 min^{-1}. During regenerative braking the maximum developed torque is -680 Nm. The stator has form wound coils with insulation class 200. Mechanical protection is IP20 (open motor), so interior of the motor is exposed to outside moisture and dirt.

The torque requirements for IPM motors for the same performance of the tram will be 50 % higher since four motors will be used. The stator is assumed to have random wound coils made of round enameled wire with H class insulation and maximum allowed hot-spot temperature of 180 °C. The motor has 8 poles. The advantages of the higher number of poles and random wound coils are significantly shorter end windings on both ends which allow longer stack length within the same overall length of the machine.

During exploitation, wheels of the tram are exposed to wear creating tiny iron particles that can stick to the rotor of the IPM motor due to attracting forces of the magnets. After a certain period of time it can fill the air gap and damage the motor. Therefore, the IPM motor needs to be built with IP55 degree of mechanical protection (totally enclosed).

The 50 % increase in power and torque is partly achieved by increasing the stack length by 31 % (327 mm vs. 250 mm) and partly by utilizing an IPM motor with inherently higher torque density than IM which is maximized by means of design optimization. An aggravating factor for the IPM motor is the IP55 mechanical protection vs. IP20 of the existing IM which reduces the effective cooling of the motor.

Based on the data provided by the manufacturer of the tram, the traction force, acceleration, tram speed and motor torque shown in Figs. 2 to 3 have been calculated. A driving cycle consists of acceleration to the maximum speed of 70 km/h followed by driving at constant maximum speed and braking to standstill. The tram is idle for 20 seconds until the start of a new cycle. The distance between two stations is 1000 m. The IPM motor must provide 705 Nm of torque during acceleration and 1020 Nm during braking.

III. Optimized Design of IPM Motor

Design of a traction motor is more complex than design of a motor for continuous duty due to intermittent load

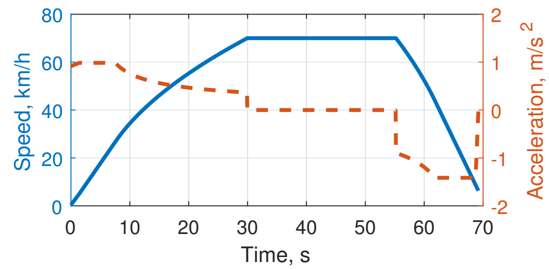

Fig. 2. Tram speed (full line, left y-axis) and acceleration (dashed line, right y-axis)

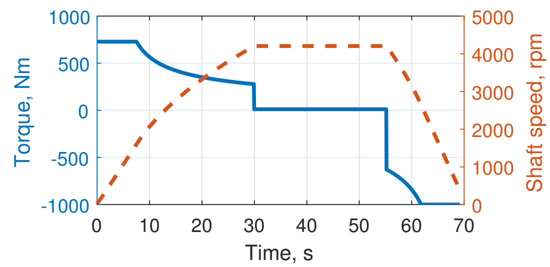

Fig. 3. Required IPM motor shaft torque (full line, left y-axis) and shaft speed (dashed line, right y-axis)

characteristics. Consideration of the entire driving cycle of the vehicle in terms of time dependence of generated power losses and the resulting heating of the motor is computationally too intensive. Therefore, the motor design is performed in four multi-physical steps:

1) Optimization of radial cross-section by maximizing the torque density of the motor within predefined constraints,
2) Verification of mechanical strength of the thin rotor bridges through finite element structural analysis,
3) Selection of the number of turns per coil and the number of parallel paths considering voltage limits and calculated thermal transient of the motor during one driving cycle,
4) Design of the cooling fan.

In this process the current density and the upper limit of linear current density constraint equal the values used in the induction motor at maximum developed torque during acceleration of the tram. The initial design constraint is that both motors have the same outer dimensions of the stator core (due to limited available space on the tram's bogie) and the same size and location of the axial cooling ducts. After finishing step 1 within these constraints, an optimal cross-section of the IPM motor is obtained which yields maximum torque density. The minimum required axial length of the lamination stack is determined by calculating the time variation of winding losses within one driving cycle of the tram which is assumed to be repeating indefinitely. This is done for an initially selected axial length. From the average value of these losses the stator current density which corresponds to the current density of the continuous duty cycle is determined. The average winding temperature with this current density in a continuous duty will be approximately equal to the average value of the time variation of winding temperature within an actual duty cycle of the tram. This average temperature is limited to 145 °C (according to class F insulation) and is calculated using thermal model of the motor implemented in Motor-CAD software [25] and the cooling air speed measured in the existing induction motor using hot wire sensor. This temperature limit also determines the minimum required axial length. In this process the number of stator winding turns per coil and parallel paths must be varied (step 3) to keep the motor within the voltage constraints of the power supply. The step 3 has been thoroughly explained in the previously published conference paper [26]. In the step 4 the new cooling fan for the IPM motor has been designed to produce the required air flow to keep the stator winding within predefined thermal constraints and its design procedure is explained in a paper accepted for conference presentation [27].

The utilization of finite element method is practically unavoidable in the case of IPM motors due to significant influence of saturation of thin iron bridges in the rotor laminations on motor performance. The FEA is computationally intensive and the optimization may require thousands of field calculations to evaluate constraint functions and cost function for all the vectors in the population and all generations. Significant time savings can be achieved if all calculations are performed using magnetostatic simulations with fixed rotor position. The detailed explanation of various approaches to calculation of IPM motor parameters and performance using only magnetostatic simulations is available in [28]. However, in the existing approach to constraint handling for the DE algorithm derived by Lampinen [29] there is room for improvement by avoiding unnecessary calculations of constraint functions. This becomes significant in the optimization problems in which evaluation of constraint functions is computationally intensive which is the case described in this paper. These improvements are explained in detail further in the paper and are included in the modified Matlab code of the DE algorithm originally presented in [30], [31].

IV. Optimization Procedure Details

Our optimization of the lamination 2D cross-section is set up as a single-objective optimization problem which is mathematically defined as:

find the vector of parameters

$$\vec{x} = [x_1, x_2, \dots, x_D],\ \vec{x} \in R^D$$

subject to D parameter constraints (boundary constraints)

$$x_i^{(L)} \leq x_i \leq x_i^{(U)}, \quad i = 1, \dots, D$$

and subject to m inequality constraints (constraint functions)

$$g_j(\vec{x}) \leq 0, \quad j = 1, \dots, m$$

which will minimize (or maximize) the function $f(\vec{x})$.

The applied optimization workflow is shown in Fig. 4. Optimization process starts with problem definition (boundaries, constraints, objectives, model type) and a preset of constant model parameters (slots, poles, winding, etc.). After entering the optimization loop, the following steps are performed iteratively:

1) optimization algorithm generates vector x
2) variables are converted to model parameters
3) model is setup (drawn)
4) model is solved
5) model performance is extracted (post-processing)
6) constraint functions and objective function values are calculated
7) constraints and objectives are passed back to the optimization algorithm

In our case, the calculation engine is a PM motor design dedicated template-based software SPEED PC-BDC [32] powered by PC-FEA finite element module, connected to Matlab via ActiveX link. Regarding the workflow in Fig 4, Model drawing and setup, Model solving and Extraction of performance are handled by SPEED PC-BDC, while all other boxes are handled through a Matlab source-code.

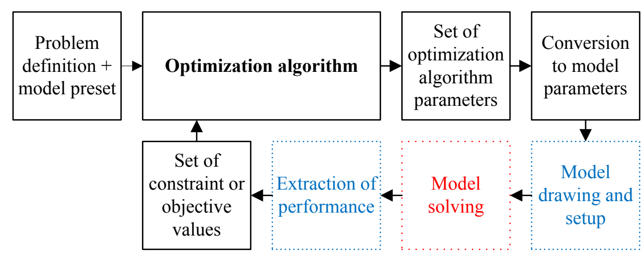

Fig. 4. Workflow for FEA based optimization [33]

A. Preset model

The number of slots and poles is selected to be 36/8 which yields a two-layer fractional slot winding with distributed overlapping coils and with good trade-off between inherent capability for mitigation of torque pulsations, susceptibility to noise and possibility of using multiple parallel paths.

Optimization was carried out with one turn per coil $n_c = 1$ and one parallel path $a_p = 1$. If current density is kept the same, the subsequent variations in winding design do not affect the amount of torque the motor develops since torque solely depends on the total ampere-turns in the slot. This approach is in accordance with the theory presented in [34], [35].

A set of parameters with constant values is listed in Table I while the parameters which are subject to optimization are listed in Table II.

B. Smart parametrization to help obtain candidates with feasible geometry

The proposed rotor geometry has two layers of permanent magnets. The layer closer to the rotor is V-shaped and contains two magnet cavities while the layer closer to the shaft is U-shaped and contains three magnet cavities. The production cost of the motor can be reasonably reduced if it is imposed that the permanent magnet bricks used in all cavities must be of equal size. Slanted cavities in the layer closer to the shaft contain two bricks while all other cavities contain a single brick.

TABLE I
IPM MOTOR CONSTANT PARAMETERS

Parameter	Value
Number of slots	36
Number of poles	8
Rated shaft speed, min^{-1}	1700
Stator outer diameter, mm	320
Stack length, mm	250
Shaft diameter, mm	70
Air gap, mm	1
Slot opening width, mm	2,5
Slot opening depth, mm	1
Coil pitch	4
Slot fill factor	0,4
RMS current density, A/mm^2	7
Permanent magnet type	NdFeB (N38EH)

TABLE II
DEFINITION OF OPTIMIZATION VARIABLES

Term	Boundaries	Explanation
D_s/D_{so}	[0.45, 0.75]	Ratio of stator inner diameter (D_s) to outer diameter (D_{so})
$d_{ys}/[(D_{so}-D_s)/2]$	[0.3, 0.7]	Ratio of yoke thickness (d_{ys}) to difference between stator outer ($D_{so}/2$) and inner radius ($D_s/2$)
b_{ts}/τ_s	[0.3, 0.7]	Ratio of tooth width b_{ts} to slot pitch τ_s at D_s
$\lambda_m = d_m/[(D_r D_{rin})/2]$	[0.1, 0.3]	Ratio of total cavity thickness (d_m) to difference between rotor outer ($D_r/2$) and inner radius ($D_{rin}/2$)
λ_{md1}	[0.2, 0.6]	Relative share of total rotor lamination depth for the outermost rotor section
λ_{md2}	[0.05, 0.4]	Relative share of total rotor lamination depth for the middle rotor section (between the cavities)
β/β_0	[0.8, 1]	Angle of slanted magnets (β) relative to the maximum feasible angle (β_0)
λ_p	[0.55, 0.95]	Angular span of the inner rotor cavity relative to the pole pitch
α	[40, 80]	Angle between magnet cavities in the outermost layer

The parameters subject to optimization have been normalized in order to minimize the occurrence of unfeasible motor geometries that would frequently emerge otherwise. This is especially noticeable in the definition of "lambda" parameters. Parameter λ_m defines the total thickness of cavities in both layers (i.e. 2 $\times$ thickness of magnet) relative to the total rotor thickness (the shortest distance between shaft and the airgap). Additional two parameters $\lambda_{md1}, \lambda_{md2}$ define the distance of the first layer from the airgap and the distance between the layers, respectively. This approach drastically reduces appearance of geometrically unfeasible candidates. Furthermore, boundaries for "lambda" parameters are always in the interval [0,1].

C. Geometrical feasibility

The term *feasibility* is usually related to the solution and it denotes that the solution satisfies all the given constraints. In other words, the region enclosed by $\forall g_j(\vec{x}) = 0$ is known as the feasible region. There is another type of feasibility, so called "geometrical or model feasibility". Geometrically feasible model is valid for solving: there are no overlapping edges, negative lengths or non-conventional geometric relations that will inevitably produce errors after start of the FE solver. This is especially important when template-based electric motor design software is used. In order to avoid drawing and creation of such non-valid model, a procedure to determine the geometrical feasibility can be performed inside the optimization algorithm. Each candidate vector is checked for geometrical feasibility. If the parameters do not pass the feasibility check, the complete set of parameters is randomly initialized again until the geometrical feasibility is achieved [33].

A smart parametrization described in section IV-B can result in a minimum amount of feasibility conditions, which helps the code to be simple and clear, but also easier to debug if there is a massive appearance of unfeasible geometric designs. Thus, feasibility conditions considered in our case are:

- all magnets must have positive lengths,
- distance between the inner cavity and the shaft should not be smaller than a predetermined value to ensure mechanical integrity of the rotor lamination in that region,
- slanted magnets should not overlap between adjacent poles. This is determined based on the location of the point S as shown in Figs. 5 and 6. The radius-vector of the point S should always be longer than outer radius of the rotor.

D. Handling of inequality constraints

Inequality constraints normally arise from different electromagnetic, thermal, mechanical, manufacturing, economic or standard limits such as maximum flux density in the stator tooth, maximum PM temperature, maximum stress in the IPM rotor bridge, minimum dimensions of magnet bricks, maximum cost of the active material, maximum noise etc. [33].

Traditional approach for handling constraint functions uses penalty functions to penalize the solutions which violate constraints. This principle is implemented in the form of weighted sums which modifies each objective function. Despite the popularity of penalty functions, they have several drawbacks the main one of which is the requirement for careful fine tuning of the penalty factors which accurately estimates the degree of penalization to be applied in order to approach the feasible region efficiently. In addition, this method can suffer from problems related to poor choice of the weight factors which can affect the convergence.

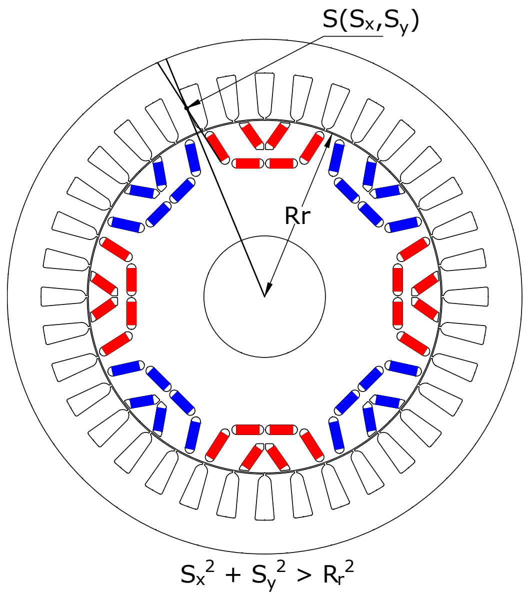

Fig. 5. Example of feasible geometry

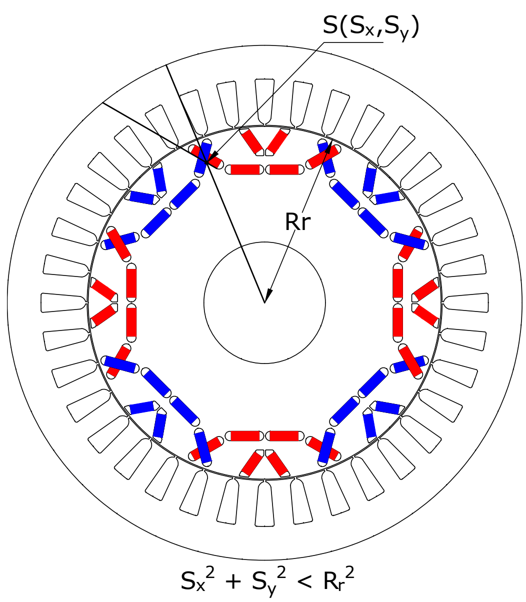

Fig. 6. Example of unfeasible geometry

Lampinen's approach [29] to efficiently handle constraint functions requires that the trial vector is selected for the new generation if:

1) it satisfies all constraints and has a lower or equal objective function value than the design from the current generation, or
2) it satisfies all constraints, while the current vector does not, or
3) neither the trial nor the current vector satisfy the constraints, however, the trial vector does not violate any constraint more than the current vector.

The main advantages of the Lampinen's approach are that it forces the selection towards feasible regions where constraints are satisfied thus resulting in faster convergence and also saves time since no evaluation of the objective function occurs if constraints are violated. However, in its original form it does not define the priorities in constraint evaluations regarding computational complexity and time duration, nor the measures for avoiding unnecessary computations when possible.

We used a specific novel approach regarding handling of the constraint inequality functions in order to reduce the overall optimization time while ensuring that the optimal solution does not violate any of the constraints. The algorithm is depicted as pseudocode Algorithm 1. It describes selection procedure between individuals (vectors) $X_{i,G}$ from the current generation G and trial individuals $U_{i,G+1}$ which compete to enter the new generation $G+1$ as individuals $X_{i,G+1}$.

Initial loop of the algorithm is used to evaluate all the constraint functions for trial members of the new generation. It is interrupted as soon as a constraint is violated. It then continues with vector evaluation according to the original Lampinen's approach. In the case when interruption occurs, further evaluation of the constraint functions for the trial member will not be necessary if the competing candidate from the previous generation does not violate any of the constraints thus saving computational time. There can also be a case when calculation of constraints was interrupted for the candidate from the previous generation while the trial member satisfies all the constraints. In that case the computational time was already saved in the past. In the end, if neither the trial nor the current vector satisfy all the constrains, evaluation of constraint functions must be continued for both vectors in order to acquire enough data to compare their overall violation of the constraints.

To summarize, computational time can be saved as shown in the line 3 of this algorithm with the condition that the propagation of the individuals to the new generation occurs according to the line 8 or line 12. This is not the case only when two unfeasible solutions are compared in order to determine which one violates the constraints (line 15) less.

E. Normalization of inequality constraints

As advised in [36], constraint functions may be of widely differing magnitudes. Such differences can make some constraint functions more sensitive than others in the optimization process, possibly leading to failures in convergence. For this reason, it is preferred to normalize all constraint functions by choosing suitable base values and expressing all quantities in per unit of those values. A preferred base value is the minimum or maximum value of the imposed constraint. This can be generally written as

$$g(\vec{x}) = \epsilon * (1 - \frac{X(\vec{x})}{X_{lim}}) \tag{1}$$

where g is the constraint function, X is the performance index of the studied object (efficiency, power factor, linear current density), X_{lim} is the limit of the performance index (minimum or maximum), while the ϵ parameter takes value 1 if the constraint is of *minimum* type, or value -1 if the constraint is of *maximum* type.

Normalization allows combining of multiple constraint functions into one single constraint function which further

Algorithm 1 Selection of vectors in generation $G+1$

for $j = 1$ to m **do**
  evaluate constraint $g_{j,i,G+1} = g_j(U_{i,G+1})$
  if a constraint is violated, i.e. $g_{j,i,G+1} > 0$ **then** do not evaluate other $g_{j+1,i,G+1} ... g_{m,i,G+1}$.
if there is no constraint violation in the current generation G, i.e. $\forall j\ g_{j,i,G} \leq 0$ **then**
  if trial vector does not violate any constraints, i.e. $\forall j\ g_{j,i,G+1} \leq 0$ **then**
    evaluate objective function $f(U_{i,G+1})$
    propagate better vector, the one with the smaller objective function value
  else *propagate the current member* $X_{i,G}$, i.e. $X_{i,G+1} \leftarrow X_{i,G}$
else if constraint violation exists in the current generation G, i.e. $\exists j\ g_{j,i,G} > 0$
  if trial vector does not violate any constraints, i.e. $\forall j\ g_{j,i,G+1} \leq 0$ **then**
    evaluate objective function $f(U_{i,G+1})$
    propagate the trial vector $U_{i,G+1}$, i.e. $X_{i,G+1} \leftarrow U_{i,G+1}$
  else if constraint violation exists in the trial generation, i.e. $\exists j\ g_{j,i,G+1} > 0$
    evaluate all unevaluated constraints in both the previous and current generation
    propagate better vector, the one with the smaller violation of the constraints

TABLE III
IPM Motor Inequality Constraints

Constraint		Description	Symbol	Limit
g_1	c_1	RMS linear current density	K	$\leq$ 55 kA
g_2	c_2	Efficiency	η	$\geq$ 0.95 %
	c_3	Total Loss	P_{loss}	$\leq$ 10 kW
	c_4	Output power at rated speed	P_{n_r}	$\geq$ 85 kW
	c_5	Power factor	$\cos\varphi$	$\geq$ 0.8
	c_6	Line-line voltage	V_{ll}	$\leq$ 440 V
g_3	c_7	Flux density in stator tooth	$B_{st,max}$	$\leq$ 1,8 T
	c_8	Flux density in stator yoke	$B_{sy,max}$	$\leq$ 1,3 T
g_4	c_9	Power at 3x rated speed	P_{3n_r}	$\geq P_{n_r}$

results in reduction of the overall optimization time. Constraint functions $c_1, c_2, ...c_n$ are combined in a final g_i constraint function through the following formulation:

$$g_i = \max(c_1, c_2, ...c_n) \tag{2}$$

Inequality constraints for this particular case are defined in Table III. The constraint function g_1 contains purely analytical and fast calculation of stator linear current density. The procedure related to constraint function g_2 contains multiple magnetostatic FEA calculations in order to find the maximum of torque vs. current phase advance curve thus determining the optimal maximum torque per ampere (MTPA) control angle through polynomial fit. A transient FEA calculation is then performed to determine the rated load point efficiency, power factor, shaft torque and terminal voltage. The constraint function g_3 consists of the calculation of maximum stator tooth and yoke flux densities which requires another FEA simulation. The constraint function g_4, however, requires a mini-optimization (*fmincon*) procedure including iterative FEA calculations in order to determine the shaft power at 3 times rated speed. This procedure has been thoroughly explained in [28] on another motor example.

F. Time savings related to the proposed method

Methodology proposed in Section IV-E and shown in Algorithm 1 was applied while performing the optimization of the PM traction motor. The benefits of this algorithm are illustrated in Fig. 7 showing cumulative number of evaluations for different g functions while performing 100 iterations of Differential Evolution algorithm with population size $NP = 30$ plotted against the number of iterations.

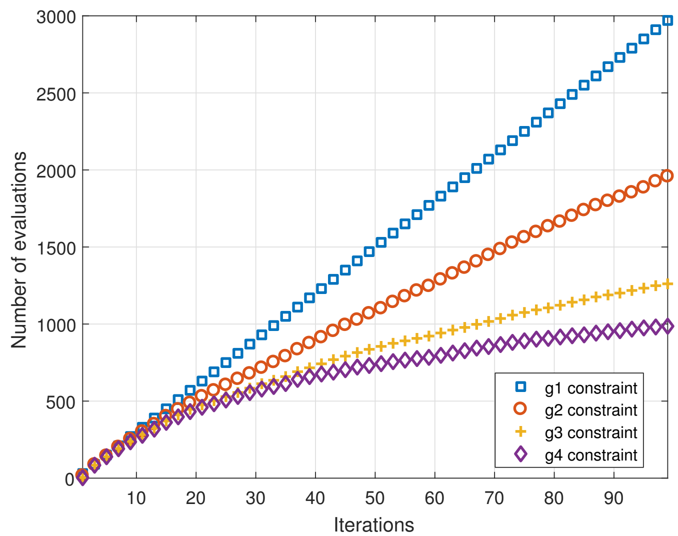

Fig. 7. Number of evaluations of constraint functions vs. number of iterations (generations) of DE algorithm

The original approach would result in each g function to be evaluated NP times for each iteration which means that all lines would overlap with the g_1 line. Our modification, which interrupts constraint evaluation, results in reduction of the number of evaluations for constraint functions g_2, g_3, g_4. Qualitatively, it is clearly shown that the number of evaluations of all g functions different from g_1 is significantly reduced. Quantitatively, the exact time savings can be calculated from the number of omitted evaluations for each constraint function and the average evaluation time for each constraint function. The average evaluation time per constraint function and the cumulative number of evaluations for 100 iterations are shown in Table IV. The proposed optimization procedure took 20.3

TABLE IV
EVALUATION TIME

Constraint	Average evaluation time, s	Number of evaluations
g1	0.1	3000
g2	21.9	1976
g3	10.9	1273
g4	16.4	991

hours while the original approach would take 40.7 hours (3000 evaluations for each constraint function) which is a significant reduction of evaluation time, close to 50 %. Not all optimization cases will have equal time saving. It is dependent on the boundaries of the optimization variables (the size of the search space), the size of the feasible space, the computational cost of the constraint functions and the rhythm of propagation towards the optimal solution. However, this method will always use the least number of evaluations needed to achieve the optimal solution by respecting constraint functions as hard constraints.

The optimization procedure was repeated multiple times and each time identical (global) optimum was achieved with very similar time savings.

V. OPTIMIZATION RESULTS

The optimization resulted in a motor geometry with the highest torque within a given stack volume which satisfies all constraints. The obtained torque density is 27.4 kNm/m^3. The radial cross-section of the optimal lamination design is shown in Fig. 8. Minor modifications of the shapes of permanent magnet cavities in the rotor have been made with respect to the standard template in PC-BDC software in order to better secure the magnet bricks in position. These modifications do not affect the electromagnetic properties of the optimal design which was verified by modeling the final design with Infolytica MagNet software [37].

The rotor was constructed with segmented skewing. Two segments have been mutually shifted by one half of the slot pitch. A round bolt was driven through the laminations at every pole pitch in the vicinity of the magnets in the outer layer in a slightly misaligned position (one quarter of the slot pitch) with respect to the centerline of the rotor cavity structure. The skewing was achieved by rotating one half of the lamination stack by 180 degrees, assembling all laminations and driving the bolt straight through the hole. In this manner two halves of the stack ended up in a mutually skewed position by one half of the slot pitch.

VI. TESTING

The designed optimal motor was manufactured as a prototype and tested in the laboratory (Fig. 10).

This motor is intended to be used on a specific driving cycle of the tram so in general it is not important to define its rated operating point for S1 continuous duty cycle [38]. However, for testing purposes it is convenient to define an equivalent S1 rated power to yield approximately equal thermal stress on the stator winding and confirm the motor's ratings in the actual intermittent operation as well. During test the motor

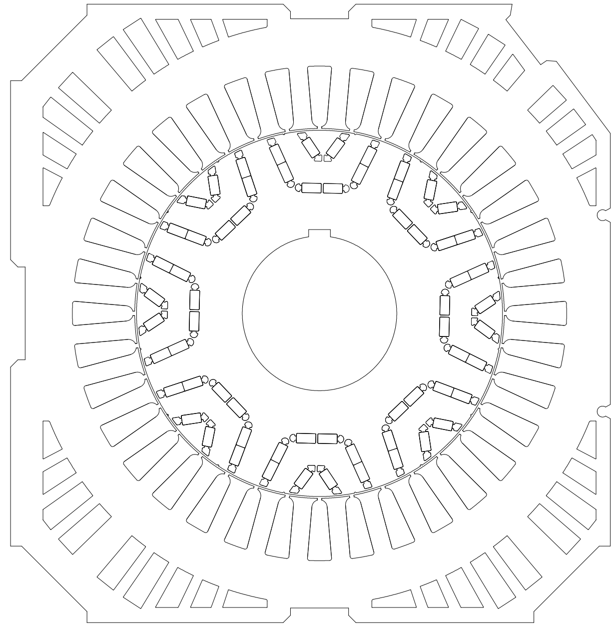

Fig. 8. Final optimized adjusted geometry with the actual lamination shape

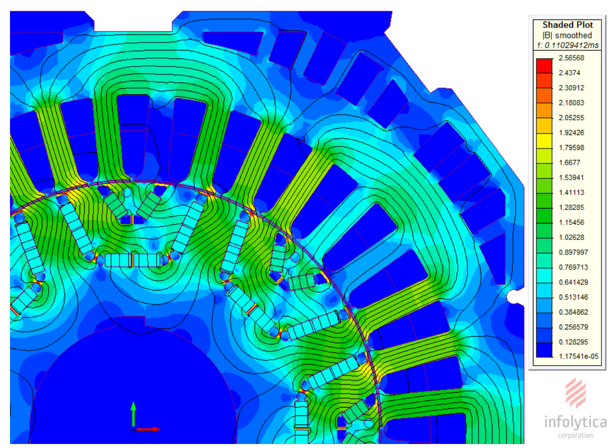

Fig. 9. Field lines and flux density shaded plot [37] for a final geometry

was loaded with a torque which is produced at a current of approximately 223 A. This current will produce copper losses which correspond to the average copper losses during a driving cycle. The average motor shaft speed during the actual driving cycle is 2380 min^{-1}. A very good match is obtained when measurements are compared to the electromagnetic calculation [37] and thermal calculation [25] as shown in Table V. It is important to mention that the characteristics of the permanent magnet material were measured in the laboratory, thus an excellent match of measured and calculated EMF was possible as shown in Fig. 11.

Measured efficiency of the prototype is 0.55 % higher than the efficiency limit for IE4 class (it has 15 % smaller total losses) which is calculated by

$$\eta_{IE4} = A[\log(T_n)]^3 + B[\log(T_n)]^3 + C[\log(T_n)] + D \quad (3)$$

where T_n is the rated torque, and coefficients A, B, C and D are defined in [39].

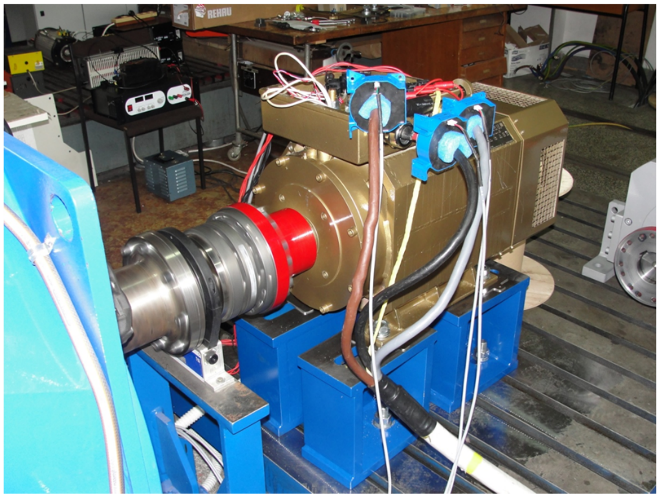

Fig. 10. IPM motor under test

TABLE V
COMPARISON OF CALCULATED AND MEASURED RESULTS

	Calculation	**Measurement**
Shaft speed, min^{-1}	2380	2380
Shaft power, kW	118,5	118,4
Shaft torque, Nm	475,6	475,0
Current, A	222,7	221,6
Efficiency, %	96,77	96,67
Total losses, kW	3,95	4,10
Winding temperature, °C	141,9	144,4
PM temperature, °C	141,2	142,7

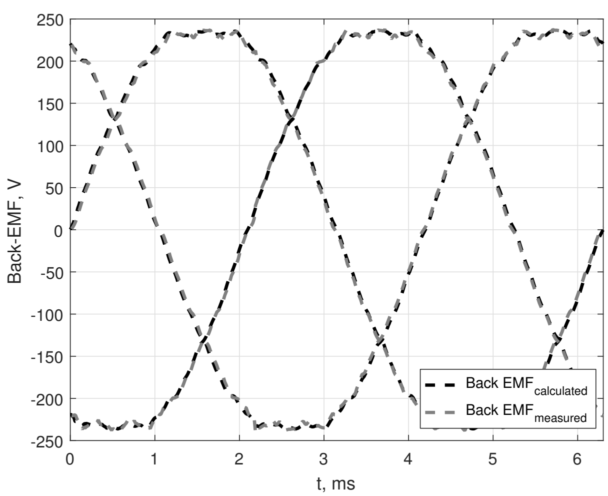

Fig. 11. Comparison of measured and calculated phase EMF at 2380 min^{-1} and ambient temperature of 23 °C

VII. CONCLUSION

An improved algorithm for handling of inequality constraints in differential evolution optimization algorithm has been presented. It complements the existing algorithm based on competition between the existing and the trial vector in terms of how well they satisfy the inequality constraints separately from evaluation of the cost function. In our improved algorithm the computationally intensive finite element based procedure for calculating the data used for evaluation of constraint functions is interrupted if the constraint is violated therefore saving computational time. The procedure can be later continued if it is required by the vector selection process. Furthermore, it is shown how to efficiently perform geometrical parametrization, setup of geometrical feasibility functions and normalization of constraints.

The overall approach is demonstrated as a case study of design optimization of a permanent magnet traction motor for a low floor city tram. An excellent match of the manufactured and tested prototype with regards to electromagnetic and thermal calculations is obtained.

ACKNOWLEDGMENT

This research was partially funded by the European Union under the project titled *Permanent Magnet Machine Technology for Boosting the Energy Efficiency in Traction and Marine Applications* (MAGEF), Contract No. IPA2007/HR/16IPO/001-040508 and partially by the Croatian Science Foundation under the project IP-11-2013-7801 *Advanced Electric Drives for Traction Applications*.

The authors also thank Končar Electric Vehicles Inc., Croatia for providing valuable data on TMK2200 tram and Motor Design Ltd., producers of Motor-CAD software, for valuable assistance in thermal modeling.

REFERENCES

[1] F. Parasiliti, M. Villani, S. Lucidi, and F. Rinaldi, "Finite-element-based multiobjective design optimization procedure of interior permanent magnet synchronous motors for wide constant-power region operation," *IEEE Transactions on Industrial Electronics*, vol. 59, no. 6, pp. 2503–2514, June 2012.

[2] M. Barcaro, N. Bianchi, and F. Magnussen, "Permanent-magnet optimization in permanent-magnet-assisted synchronous reluctance motor for a wide constant-power speed range," *IEEE Transactions on Industrial Electronics*, vol. 59, no. 6, pp. 2495–2502, June 2012.

[3] H. I. Lee and M. D. Noh, "Optimal design of radial-flux toroidally wound brushless dc machines," *IEEE Transactions on Industrial Electronics*, vol. 58, no. 2, pp. 444–449, Feb 2011.

[4] G. Lei, J. G. Zhu, Y. G. Guo, J. F. Hu, W. Xu, and K. R. Shao, "Robust design optimization of pm-smc motors for six sigma quality manufacturing," *IEEE Transactions on Magnetics*, vol. 49, no. 7, pp. 3953–3956, July 2013.

[5] W. Q. Chu, Z. Q. Zhu, and J. T. Chen, "Simplified analytical optimization and comparison of torque densities between electrically excited and permanent-magnet machines," *IEEE Transactions on Industrial Electronics*, vol. 61, no. 9, pp. 5000–5011, Sept 2014.

[6] H. M. Hasanien, "Particle swarm design optimization of transverse flux linear motor for weight reduction and improvement of thrust force," *IEEE Transactions on Industrial Electronics*, vol. 58, no. 9, pp. 4048–4056, Sept 2011.

[7] J. A. Tapia, J. Pyrhonen, J. Puranen, P. Lindh, and S. Nyman, "Optimal design of large permanent magnet synchronous generators," *IEEE Transactions on Magnetics*, vol. 49, no. 1, pp. 642–650, Jan 2013.

[8] J. A. Tapia, A. Parviainen, J. Pyrhnen, P. Lindh, and R. R. Wallace, "Optimal design procedure for an external rotor permanent-magnet machine," in *2012 XXth International Conference on Electrical Machines*, Sept 2012, pp. 2695–2701.

[9] L. Alberti, N. Bianchi, A. Boglietti, and A. Cavagnino, "Core Axial Lengthening As Effective Solution To Improve The Induction Motor Efficiency Classes," *IEEE Transactions On Industry Applications*, vol. 50, no. 1, pp. 218–225, Jan 2014.

[10] A. Boglietti, A. Cavagnino, L. Ferraris, M. Lazzari, and G. Luparia, "No Tooling Cost Process For Induction Motors Energy Efficiency Improvements," *IEEE Transactions On Industry Applications*, vol. 41, no. 3, pp. 808–816, May 2005.

[11] G. Bramerdorfer, A. Cavagnino, and S. Vaschetto, “Impact of im pole count on material cost increase for achieving mandatory efficiency requirements,” in *IECON 2016 - 42nd Annual Conference of the IEEE Industrial Electronics Society*, Oct 2016, pp. 1680–1685.
[12] E. B. Agamloh, A. Boglietti, and A. Cavagnino, “The incremental design efficiency improvement of commercially manufactured induction motors,” *IEEE Transactions on Industry Applications*, vol. 49, no. 6, pp. 2496–2504, Nov 2013.
[13] European Commission, “Implementing Directive 2005/32/EC Of The European Parliament And Of The Council With Regard To Ecodesign Requirements For Electric Motors,” *Official Journal Of The European Union*, no. 191, pp. 26–34, July 2009.
[14] U. S. E. P. Agency, “EPAct USA Energy Policy Act,” [1.10.2013.]. [Online]. Available: http://www.epa.gov/lawsregs/laws/epa.html
[15] G. Pellegrino, F. Cupertino, and C. Gerada, “Automatic design of synchronous reluctance motors focusing on barrier shape optimization,” *IEEE Transactions on Industry Applications*, vol. 51, no. 2, pp. 1465–1474, March 2015.
[16] C. Lu, S. Ferrari, and G. Pellegrino, “Two design procedures for pm synchronous machines for electric powertrains,” *IEEE Transactions on Transportation Electrification*, vol. PP, no. 99, pp. 1–1, 2017.
[17] D. Ionel and M. Popescu, “Ultrafast Finite-Element Analysis Of Brushless PM Machines Based On Space-Time Transformations,” *IEEE Transactions On Industry Applications*, vol. 47, no. 2, pp. 744–753, March 2011.
[18] P. Zhang, G. Sizov, J. He, D. Ionel, and N. Demerdash, “Calculation Of Magnet Losses In Concentrated-Winding Permanent-Magnet Synchronous Machines Using A Computationally Efficient Finite-Element Method,” *IEEE Transactions On Industry Applications*, vol. 49, no. 6, pp. 2524–2532, Nov 2013.
[19] G. Y. Sizov, D. M. Ionel, and N. A. O. Demerdash, “A review of efficient fe modeling techniques with applications to pm ac machines,” in *2011 IEEE Power and Energy Society General Meeting*, July 2011, pp. 1–6.
[20] ——, “Modeling and parametric design of permanent-magnet ac machines using computationally efficient finite-element analysis,” *IEEE Transactions on Industrial Electronics*, vol. 59, no. 6, pp. 2403–2413, June 2012.
[21] P. Zhang, G. Y. Sizov, D. M. Ionel, and N. A. O. Demerdash, “Establishing the relative merits of interior and spoke-type permanent-magnet machines with ferrite or ndfeb through systematic design optimization,” *IEEE Transactions on Industry Applications*, vol. 51, no. 4, pp. 2940–2948, July 2015.
[22] G. Y. Sizov, P. Zhang, D. M. Ionel, N. A. O. Demerdash, and M. Rosu, “Automated multi-objective design optimization of pm ac machines using computationally efficient fea and differential evolution,” *IEEE Transactions on Industry Applications*, vol. 49, no. 5, pp. 2086–2096, Sept 2013.
[23] G. Bramerdorfer, A. C. Zvoianu, S. Silber, E. Lughofer, and W. Amrhein, “Possibilities for speeding up the fe-based optimization of electrical machines; a case study,” *IEEE Transactions on Industry Applications*, vol. 52, no. 6, pp. 4668–4677, Nov 2016.
[24] A. M. El-Refaie, “Motors/generators for traction/propulsion applications: A review,” *IEEE Vehicular Technology Magazine*, vol. 8, no. 1, pp. 90–99, March 2013.
[25] Motor Design Ltd., “Motor-CAD / Motor-LAB software.” [Online]. Available: http://www.motor-design.com/motorlab.php
[26] M. Martinovic, D. Zarko, S. Stipetic, T. Jercic, M. Kovacic, Z. Hanic, and D. Staton, “Influence of winding design on thermal dynamics of permanent magnet traction motor,” in *International Symposium on Power Electronics, Electrical Drives, Automation and Motion (SPEEDAM), 2014*, June 2014, pp. 397–402.
[27] T. Jercic, D. Zarko, M. Martinovic, M. Kovacic, J. Juric, Z. Hanic, and S. Stipetic, “Centrifugal fan design for permanent magnet synchronous motor in a traction application,” in *Accepted for presentation at 2017 International Electric Machines and Drives Conference (IEMDC 2017)*, Sept 2017.
[28] S. Stipetic, D. Zarko, and M. Kovacic, “Optimised design of permanent magnet assisted synchronous reluctance motor series using combined analytical-finite element analysis based approach,” *IET Electric Power Applications*, vol. 10, no. 5, pp. 330–338, 2016.
[29] J. Lampinen, “Multi-Constrained Nonlinear Optimization By The Differential Evolution Algorithm,” in *6th On-Line World Conference On Soft Computing In Industrial Applications (Wsc6)*, 2001, pp. 1–19.
[30] K. Price, R. M. Storn, and J. A. Lampinen, *Differential evolution: a practical approach to global optimization*. Springer Science & Business Media, 2006.
[31] K. Price and R. Storn, “Matlab code for differential evolution.” [Online]. Available: http://www1.icsi.berkeley.edu/ storn/code.html
[32] Siemens, “SPEED Software Suite.” [Online]. Available: http://www.speed-emachine-design.com/
[33] S. Stipetic, W. Miebach, and D. Zarko, “Optimization in design of electric machines: Methodology and workflow,” in *2015 Intl Conference on Optimization of Electrical Electronic Equipment (OPTIM)*, Sept 2015, pp. 441–448.
[34] D. Zarko and S. Stipetic, “Criteria For Optimal Design Of Interior Permanent Magnet Motor Series,” in *XXth International Conference On Electrical Machines (ICEM), 2012*, Sept 2012, pp. 1242–1249.
[35] S. Stipetic, D. Zarko, and M. Popescu, “Ultra-fast axial and radial scaling of synchronous permanent magnet machines,” *IET Electric Power Applications*, vol. 10, no. 7, pp. 658–666, 2016.
[36] X. Liu and G. Slemon, “An Improved Method of Optimization for Electrical Machines,” *IEEE Transactions on Energy Conversion*, vol. 6, no. 3, pp. 492–496, Sep 1991.
[37] Infolytica, “MagNET software.” [Online]. Available: http://www.infolytica.com/en/products/magnet/
[38] IEC, “International Standard IEC/EN 60034-1 (1996) Rotating electrical machines - Part 1: Rating and performance,” 1996.
[39] ——, “International Standard IEC/EN 60034-31 (2009), Rotating electrical machines - Part 31: Selection of energy-efficient motors including variable speed applications - Application guide,” 2009.

Damir Zarko was born in Zagreb, Croatia. He received the Dipl. Eng. and M.Sc. degrees in electrical engineering from the University of Zagreb, Croatia in 1995 and 1999 respectively and the Ph.D. degree from the University of Wisconsin-Madison, Madison, WI, USA in 2004. Currently he is a Full Professor at the University of Zagreb Faculty of Electrical Engineering and Computing, Department of Electrical Machines Drives and Automation, Croatia where his research activities are related to design, modeling, analysis and optimization of electrical machines and power transformers.

Stjepan Stipetic was born in Ogulin, Croatia. He received Dipl.Eng. degree and Ph.D. in electrical engineering from the University of Zagreb, Croatia, in 2008 and 2014, respectively. Currently he is an Assistant Professor at the University of Zagreb Faculty of Electrical Engineering and Computing, Department of Electrical Machines Drives and Automation, Croatia where his research activities are related to design, modeling, analysis and optimization of electrical machines.

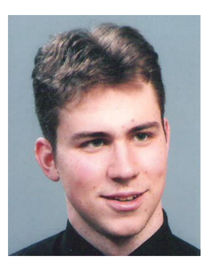

Marijan Martinovic was born in Pakrac, Croatia. He received B.S. and M.S. degrees from the University of Zagreb, Croatia in 2010 and 2013. He is currently employed in Elaphe Propulsion Technologies in Ljubljana as designer of electrical machines for electric cars. His main areas of research interest are design, modeling, analysis and optimization of electrical machines.

Marinko Kovacic was born in Split, Croatia. He received the Dipl.Eng. degree in electrical engineering from the University of Zagreb, Croatia, in 2009, where he is currently working towards the Ph.D. degree as a Research Assistant at the University of Zagreb Faculty of Electrical Engineering and Computing, Department of Electrical Machines Drives and Automation. His research interests include multilevel power converter topologies, power electronics control systems and modeling of electromagnetic components.

Tino Jercic was born in Zagreb, Croatia. He received B.S. and M.S. degrees from the University of Zagreb, Croatia in 2010 and 2012, respectively. He is currently a research associate at the University of Zagreb Faculty of Electrical Engineering and Computing, Department of Electrical Machines Drives and Automation, Croatia. His research interests include design and control of electrical machines.

Zlatko Hanic was born in Zagreb, Croatia. He received Dipl.Eng. degree and Ph.D. in electrical engineering from the University of Zagreb, Croatia, in 2009 and 2017, respectively. He is currently working as a PostDoc at the University of Zagreb Faculty of Electrical Engineering and Computing, Department of Electrical Machines Drives and Automation, Croatia. His research interests include modeling, analysis, design and optimization of electrical machines as well as electromagnetic and electromechanical devices.